Published OnlineFirst May 11, 2010; DOI: 10.1158/1078-0432.CCR-10-0026

Imaging, Diagnosis, Prognosis

Clinical Cancer Research

Tumor Metabolism and Blood Flow as Assessed by Positron Emission Tomography Varies by Tumor Subtype in Locally Advanced Breast Cancer

Jennifer M. Specht[1], Brenda F. Kurland[5], Susan K. Montgomery[3], Lisa K. Dunnwald[2], Robert K. Doot[2], Julie R. Gralow[1], Georgina K. Ellis[1], Hannah M. Linden[1], Robert B. Livingston[6], Kimberly H. Allison[4], Erin K. Schubert[2], and David A. Mankoff[2]

Abstract

Purpose: Dynamic positron emission tomography (PET) imaging can identify patterns of breast cancer metabolism and perfusion in patients receiving neoadjuvant chemotherapy (NC) that are predictive of response. This analysis examines tumor metabolism and perfusion by tumor subtype.

Experimental Design: Tumor subtype was defined by immunohistochemistry in 71 patients with locally advanced breast cancer undergoing NC. Subtype was defined as luminal [estrogen receptor (ER)/progesterone receptor (PR) positive], triple negative [TN; ER/PR negative, human epidermal growth factor receptor 2 (HER2) negative], and HER2 (ER/PR negative, HER2 overexpressing). Metabolic rate (MRFDG) and blood flow (BF) were calculated from PET imaging before NC. Pathologic complete response (pCR) to NC was classified as pCR versus other.

Results: Twenty-five (35%) of 71 patients had TN tumors; 6 (8%) were HER2 and 40 (56%) were luminal. MRFDG for TN tumors was on average 67% greater than for luminal tumors (95% confidence interval, 9-156%) and average MRFDG/BF ratio was 53% greater in TN compared with luminal tumors (95% confidence interval, 9-114%; $P < 0.05$ for both). Average BF levels did not differ by subtype ($P = 0.73$). Most luminal tumors showed relatively low MRFDG and BF (and did not achieve pCR); high MRFDG was generally matched with high BF in luminal tumors and predicted pCR. This was not true in TN tumors.

Conclusion: The relationship between breast tumor metabolism and perfusion differed by subtype. The high MRFDG/BF ratio that predicts poor response to NC was more common in TN tumors. Metabolism and perfusion measures may identify subsets of tumors susceptible and resistant to NC and may help direct targeted therapy. *Clin Cancer Res; 16(10); 2803–10. ©2010 AACR.*

Genomic profiling has identified different molecular subtypes of breast cancer, including basal-like, human epidermal growth factor receptor 2 (HER2) positive, luminal A, and luminal B (1–3). These molecular subtypes may be approximated by standard immunohistochemistry (IHC) as follows (2): basal-like (triple negative, TN) as estrogen receptor (ER) negative, progesterone receptor (PR) negative, and HER2 negative; HER2 like as ER negative, PR negative, and HER2 overexpressing; luminal A is ER and/or PR positive, HER2 negative; and luminal B is ER and/or PR positive, HER2 overexpressing. Differential response to neoadjuvant chemotherapy (NC) has been observed among breast cancer subtypes defined by either IHC (2) or by molecular profiling (4). Despite higher rates of pathologic complete response (pCR) to NC, basal and HER2 subtypes are more likely to recur, often rapidly, more often with brain and visceral metastases, and have poorer prognoses than do luminal subtypes (2, 3, 5–8). A greater understanding of the biological basis of these clinical observations may elucidate factors contributing to therapeutic responsiveness and resistance, and ultimately lead to more individualized and tumor-specific treatments.

Functional imaging of tumor blood flow (BF) and metabolism, using [^{15}O]-water and [^{18}F]-FDG positron emission tomography (PET), respectively, has been studied in breast and other tumor types (9–13, 35). Studies at this institution have shown that BF and metabolism in locally advanced breast cancer (LABC) are highly variable and provide a means of predicting response and disease relapse in patients receiving NC for LABC (9–11). Specifically, we found that LABC tumors with a pretherapy flow-metabolism mismatch [high metabolic rate of FDG (MRFDG) to BF] were more resistant to therapy, predicting

Authors' Affiliations: [1]Medical Oncology and [2]Nuclear Medicine, Departments of [3]Medicine and [4]Pathology, University of Washington, Seattle, Washington; [5]Clinical Statistics, Fred Hutchinson Cancer Research Center, Seattle, Washington; and [6]Medicine, Arizona Cancer Center, Tucson, Arizona

Corresponding Author: Jennifer M. Specht, University of Washington, Division of Medical Oncology, Seattle Cancer Care Alliance, 825 Eastlake Avenue East, G3-630, Seattle, WA 98109. Phone: 206-288-6889; Fax: 206-288-2054; E-mail: jspecht@uw.edu.

doi: 10.1158/1078-0432.CCR-10-0026

Published OnlineFirst May 11, 2010; DOI: 10.1158/1078-0432.CCR-10-0026

Translational Relevance

Locally advanced breast cancers differ in response to neoadjuvant chemotherapy (NC). Dynamic PET imaging, used to measure glucose metabolism and blood flow (BF), has been shown to provide additional prognostic information beyond clinical features such as tumor size and nodal involvement, predicting pathologic complete response, overall, and disease-free survival. Using positron emission tomography imaging conducted before NC, our study shows that the rate of glucose metabolism and the ratio of glucose metabolism to perfusion differ across breast cancer subtypes. In addition, we observed the heterogeneity of tumor BF and metabolism within the triple-negative subtype. This heterogeneity underscores the importance of further examination of the biological differences within and across tumor subtypes, as a potential means to individualize therapy for those tumors showing susceptibility or resistance to NC.

a low likelihood of pCR and a high likelihood of early relapse (10, 14). Additionally, resistant tumors were more likely to have a higher perfusion rate over the course of therapy, failure to diminish tumor perfusion at midtherapy-predicted poor response, early relapse, and death (9, 11). In multivariable models, PET measures predicted relapse and survival independently of other established prognostic measures (15–17) including primary tumor pCR and post-therapy pathologic nodal status (14). Similar associations between flow-metabolism mismatch and more aggressive tumor biology have been observed in other tumor types using functional PET imaging (12, 13, 18).

To investigate patterns of BF and glucose metabolism for different breast cancer subtypes, we analyzed PET measures of tumor glucose metabolism and BF in a cohort of patients with LABC and approximated intrinsic subtype using standard IHC criteria. At least one other study has looked at FDG uptake by breast cancer subtype (19); however, to our knowledge, this is one of the first studies to use functional imaging to investigate the relationship between tumor BF and metabolism by breast cancer subtype. Functional imaging using dynamic PET offers a unique opportunity to study tumor physiology *in vivo* and may provide a portrait of tumor physiology that is complementary to differences in patterns of gene expression measured by genomic profiling. Noninvasive functional imaging by PET may identify patterns of metabolism and BF associated with responsive and resistant tumors that may ultimately allow for the selection of cytotoxic and biological therapies based on *in vivo* tumor biology.

Materials and Methods

Patient selection. Patients presenting to the University of Washington Breast Cancer Specialty Clinic with histologically confirmed breast carcinoma scheduled to undergo NC were eligible for the study. Patients were clinically staged according the American Joint Committee on Cancer tumor-node-metastasis classification of malignant tumors (20, 21). The majority of patients presented with clinical staging consistent with LABC, but a strict definition of inoperable LABC, was not required for inclusion in this analysis. Seven patients in this cohort presented with inflammatory breast cancer as determined by clinical staging on presentation. The enrollment period was from November 1995 through December 2005. Patients were excluded if they were pregnant, unwilling, or unable to undergo PET examinations. Patients were also excluded if they were not surgical candidates. A total of 71 patients were identified with baseline [^{15}O]-water and [^{18}F]-FDG PET imaging, demographic and tumor information, and pathologic response for inclusion in this study. Analyses done on a subset of this cohort have been previous published (9–11), but did not examine molecular subtype as currently defined. Written informed consent for PET studies and follow-up was obtained according to the University of Washington Human Subjects Committee guidelines.

Definition of immunohistochemical subtypes. According to institutional standards, tumor tissue was sampled under ultrasound or stereotactic guidance for diagnosis before initiation of NC. Tumor subtype by IHC was assessed on diagnostic biopsy material. ER expression was assessed using the 1D5 antibody (DAKO) and was expressed as negative (<5%), 1+ (>5-20% of tumor cells were ER positive), 2+ (20-80% positive), or 3+ (>80% positive). PR expression was assessed using the PR88 antibody (BioGenex) and the level of expression was scored in a fashion identical to that for ER. HER2 was defined as positive if IHC showed 3+. It was considered negative in those tumors scoring 1+. For those tumors with a 2+ score on IHC, gene amplification using fluorescence *in situ* hybridization was used to determine HER2 status. HER2 was considered positive if the ratio of HER2 gene copies to chromosome 17 signals was >2. Cellular proliferation was assessed by measurement of Ki-67 antigen by monoclonal antibody (DAKO) with scoring by institutional standards as low (<10%), intermediate (10-20%), and high (>20%). Tumor grade was based on expert breast pathology review.

TN, or basal, subtype was defined as ER and PR negative without HER2 overexpression by IHC or amplification by fluorescence *in situ* hybridization. Luminal tumors were defined as those expressing either ER or PR, without regard to HER2 status. For the purposes of this analysis, luminal A and B were not subdivided. HER2-like tumors were ER and PR negative with HER2 overexpression or gene amplification.

Positron emission tomography. PET radiotracer production, imaging methods, and data analysis have been previously described (9–11, 22–24). Briefly, images were acquired on an Advance PET scanner (General Electric Medical Systems) and reconstructed by filtered back projection with an approximate resolution of 10 to 12 mm

Published OnlineFirst May 11, 2010; DOI: 10.1158/1078-0432.CCR-10-0026

(22, 23). For [^{15}O]-water studies, patients received 724 to 1,902 MBq in a 1- to 4-mL volume through bolus i.v. injection. Dynamic images were acquired for 7.75 minutes after injection. For [^{18}F]-FDG studies, 218 to 396 MBq was infused over 2 minutes in a 7- to 10-mL volume, and dynamic images were acquired for 60 minutes after the start of infusion. Regions of interest measuring mean uptake were 1.5-cm diameter circles drawn on three adjacent slices over the left ventricle and the portion of the tumor with maximal uptake on summed [^{18}F]-FDG images. Regions of interest from the summed [^{18}F]-FDG images were copied onto the corresponding dynamic [^{18}F]-FDG and [^{15}O]-water images to determine BF and tumor time-activity curves. BF estimates from [^{15}O]-water and [^{18}F]-FDG kinetic parameter estimates (MRFDG and K_1) were obtained using a model optimization software (Berkley Madonna) as previously reported (24). The measurement error of these parameters has been previously estimated as 13% for BF, 11% for FDG K_1, and 3% for K_i, in which MRFDG equals K_i multiplied by the glucose concentration (24).

Statistical analysis. Descriptive displays and linear regression analysis were used to explore how functional parameters differed by subtype. Imaging parameters were log transformed to satisfy the normality assumptions for regression analysis. Overall statistical significance of subtype (three levels) as a predictor was assessed using likelihood ratio tests. Pairwise comparisons between subtypes used the Tukey-Kramer test to control for multiple comparisons. Multivariable models were fit to examine the relationship between subtype and imaging parameters, holding tumor grade constant. Relationships among subtype, tumor grade, and proliferation (Ki-67) were assessed using Fisher's exact test. Logistic regression models were fit to describe the associations between functional parameters and response to chemotherapy, for subgroups defined by subtype. Statistical analyses were conducted using the SAS/STAT software version 9.1 (SAS Institute, Inc.) and R version 2.8.1 (R Foundation for Statistical Computing).

Results

Table 1 shows patient characteristics of the entire cohort of 71 patients with LABC. The average age at diagnosis was 47 years (range, 30-76). The majority of patients were diagnosed with infiltrating ductal carcinoma. Seven patients in this cohort presented with inflammatory breast cancer; five tumors were TN and two were HER2 like. The average tumor size was 4.9 cm (range, 1.1-14 cm). Most tumors did not overexpress the Her2/*neu* oncogene. By IHC, 25 of 71 (35%) patients had TN tumors, 6 (8%) had HER2 positive, and 40 (56%) were of the luminal subtype.

The majority of patients (n = 64, 90%) received institutional standard weekly metronomic doxorubicin with daily oral cyclophosphamide or other doxorubicin-based regimens. Doxorubicin and cyclophosphamide was followed by paclitaxel in 24 of 64 (38%) patients. Other chemotherapy regimens included cyclophosphamide, methotrexate, and 5-fluorouracil in four (6%); paclitaxel and trastuzumab in one; paclitaxel and vinorelbine in one; and docetaxel and vinorelbine in one. The mean chemotherapy duration was 18 weeks (range, 8-38 wk). Fifty-seven (80%) patients underwent mastectomy; 14 (20%) patients underwent lumpectomy of the primary breast

Table 1. Selected characteristics among patients with LABC

Characteristics	No. of patients (n = 71)	%
Age, y		
<40	19	27
40-49	25	35
50-59	19	27
≥60	8	11
Race		
Non-Hispanic white	56	79
African-American	9	13
Asian/Pacific Islander	6	8
Histology		
Ductal	65	92
Lobular	6	8
Clinical tumor classification		
T1	3	4
T2	14	20
T3	41	58
T4	13	18
Clinical lymph node classification		
N0	15	21
N1	43	61
N2	11	15
N3	2	3
Tumor size, cm		
0-1.9	5	7
2.0-5	35	49
>5	31	44
Ki-67 proliferative index*		
Low or intermediate (≤20%)	16	26
High (>20%)	45	74
Menopausal status		
Pre	47	66
Post	24	34
Tumor grade		
1	5	7
2	22	31
3	44	62
Breast cancer subtype (by IHC)		
TN	25	35
HER2	6	8
Luminal	40	56

*Unknown, n = 10.

Published OnlineFirst May 11, 2010; DOI: 10.1158/1078-0432.CCR-10-0026

tumor. Surgical management of the axillary nodes was per institutional standard with 68 (96%) of patients having an axillary node dissection.

Table 2 summarizes tumor characteristics by subtype. TN tumors were more likely to be grade 3 (odds ratio, 8.7; $P < 0.001$) and more likely to have a high Ki-67 index (odds ratio, 11.4; $P = 0.009$), compared with luminal tumors. Rates of pCR (28% for TN, 13% for luminal) were not significantly different (odds ratio, 2.7; $P = 0.19$) but were similar to pCR rates reported by others (2, 4, 8, 36).

Functional imaging parameters by subtype are described in Table 2. These data are displayed in full in Figs. 1 to 3, with boxplots overlaid to show the median and quartile values. Figure 1 shows MRFDG values before NC. MRFDG differed by subtype ($P = 0.009$), although the global effect of subtype was no longer statistically significant at the 0.05 level when controlling for tumor grade ($P = 0.07$). In both models (univariate and controlling for tumor grade), MRFDG for TN disease was on average 67% greater than for lesions with a luminal subtype [95% confidence interval (95% CI), 9-156%]. Mean FDG uptake by standardized uptake value normalized by body weight showed similar effect with standardized uptake value of TN tumors 54% greater on average than for the luminal subtype (95% CI, 10-116%; data not shown). Figure 2 shows the distribution of breast tumor BF. The subtypes did not differ in average BF levels ($P = 0.73$). Figure 3 shows that like MRFDG, the MRFDG/BF ratio differed between subtypes ($P = 0.004$). The difference persisted when controlling for tumor grade ($P = 0.03$). Pairwise comparisons found that the average MRFDG/BF ratio was 53% greater in TN compared with luminal cases (95% CI, 9-114%) and 88% greater in TN compared with HER2 (95% CI, 3-242%).

Phenotypic differences in the relationship between tumor metabolism and BF are suggested by Fig. 4, which plots MRFDG against BF and denotes patients who achieved pCR by darker plotting characters. Breast cancers of the luminal subtype with relatively high metabolism were observed to have correspondingly higher BF. The correlation of log-transformed MRFDG and BF was 0.66 ($P < 0.001$) in luminal tumors. Higher MRFDG was also associated with higher BF in TN tumors ($r = 0.64$, $P < 0.001$). However, although the strength of the relationship was similar ($r = 0.65$ for both luminal and TN), there was evidence for a difference in magnitude or slope ($P = 0.07$). When MRFDG was doubled, the predicted BF was 42% greater in luminal tumors, but only 30% greater in TN tumors (in a model constrained to have similar predicted BF for the lowest observed MRFDG for TN tumors, 2.73 μmol/min/100 g).

Figure 4 also suggests that the relationships between metabolism, BF, and pathologic response differ by subtype.

Table 2. Tumor characteristics and PET parameters by subtype

Characteristics	TN ($n = 25$)	HER2 ($n = 6$)	Luminal $n = 40$	P global difference by subtype*	Odds ratio, P TN vs luminal†
Tumor grade					
3 (vs 1 or 2)‡	22 (88%)	4 (67%)	18 (45%)		8.7
95% CI§	(70%, 96%)	(30%, 90%)	(31%, 60%)	0.001	<0.001
Ki-67 proliferative index‖					
High (vs low or intermediate)	20 (95%)	3 (60%)	22 (63%)	0.01	11.4
95% CI§	(77%, 100%)	(23%, 88%)	(46%, 77%)		0.009
PCR					
pCR (vs no or partial response)	7 (28%)	4 (67%)	5 (13%)	0.014	2.7
95% CI§	(14%, 48%)	(30%, 90%)	(5%, 26%)		0.188
MRFDG, μmol/min/100 g					
Mean	15.9	7.58	9.72	0.009	0.019
SD	10.4	5.31	7.8		
BF, mL/min/g					
Mean	0.354	0.315	0.352	0.731	0.773
SD	0.148	0.129	0.214		
MRFDG: BF ratio					
Mean	44.3	24.1	28.7	0.004	0.011
SD	23	14.6	14.6		

*Fisher's exact test for grade, Ki-67, pCR; likelihood ratio test for PET.

†Odds ratio and Fisher's exact test P value for grade, Ki-67, and pCR; Tukey-Kramer test for PET (difference not given for log-transformed variables).

‡Five luminal tumors were grade 1; others were grade 2.

§CIs computed using Wilson (score) method.

‖Missing values, $n = 4$ (TN), $n = 1$ (Her2), and $n = 5$ (luminal).

Published OnlineFirst May 11, 2010; DOI: 10.1158/1078-0432.CCR-10-0026

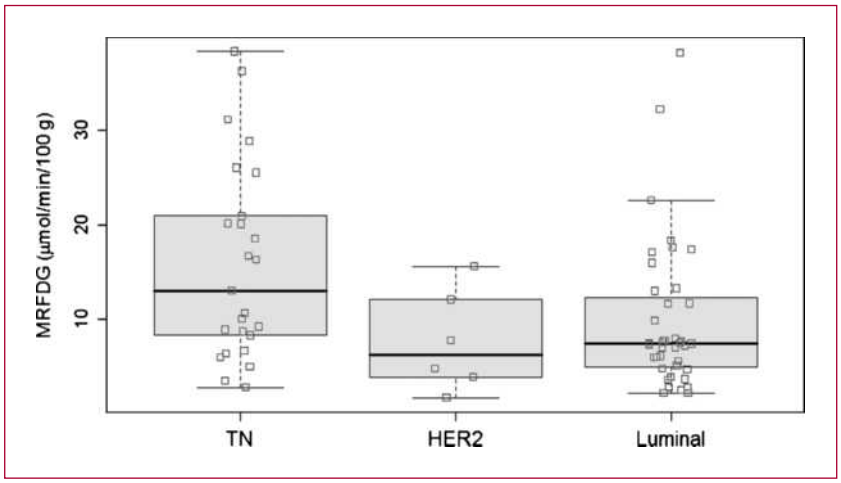

Fig. 1. MRFDG (μmol/min/100 g) by subtype using box and whisker plots. □, data points.

The majority of luminal tumors had relatively low MRFDG and BF, and did not achieve pCR following NC. When MRFDG was higher, typically in the more proliferative luminal tumors, there was a matched elevation in BF and pCR occurred frequently. In the luminal subtype, there were greater odds of pCR for patients with high BF compared with patients whose tumors had lower BF (P = 0.009) and a trend for higher MRFDG to be associated with pCR (P = 0.055). For the TN subtype, pCR was not found to be associated with MRFDG (P = 0.38), BF (P = 0.75), or the MRFDG/BF ratio (P = 0.19), although five of seven pCRs occurred in TN tumors with lower MRFDG to BF ratios.

Discussion

Using functional imaging of tumor metabolism and BF measured by [^{18}F]-FDG and [^{15}O]-water PET, this study shows that tumor BF and metabolism differ across breast cancer tumor subtypes. This is congruent with the molecular heterogeneity across tumor types identified by gene profiling (1, 3). MRFDG differed significantly between TN tumors and luminal tumors, with MRFDG being higher in the TN tumors. Similar results were found by Basu et al. (19) who reported enhanced FDG uptake measured by functional PET imaging in TN tumors. Our results add to this prior report by examining BF and the relationship between glucose metabolism and BF among different breast cancer subtypes.

The TN subtype tumors show greater variability in MRFDG than that of the luminal and HER2 subtype, suggesting heterogeneity within the TN subtype. There was no significant difference in BF across subtypes, but the relationship between metabolism and BF, expressed as the MRFDG/BF ratio, was significantly different in luminal versus TN tumors. For example, over the entire group of tumors, both MRFDG and BF varied considerably: MRFDG ranged from 0 to 40 μmol/min/100 g and BF ranged from 0 to 1 mL/min/g. Although over one third of the TN tumors had MRFDG greater than the midpoint of the range (20 μmol/min/100 g), only two of these nine

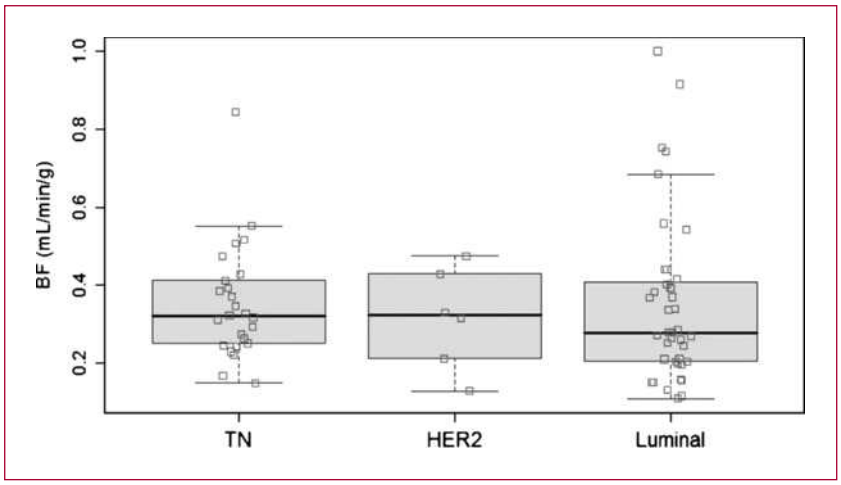

Fig. 2. BF (mL/min/g) by subtype using box and whisker plots. □, data points.

Published OnlineFirst May 11, 2010; DOI: 10.1158/1078-0432.CCR-10-0026

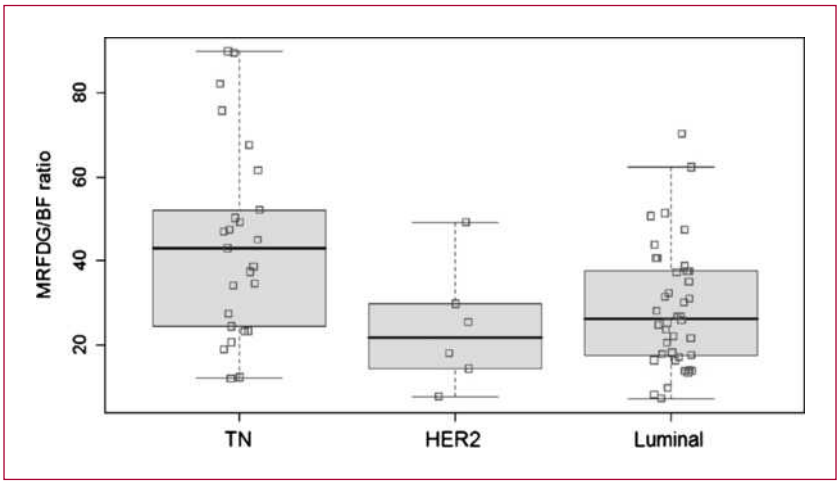

Fig. 3. MRFDG/BF ratio by subtype using box and whisker plots. □, data points.

tumors had BF over the range midpoint (0.5 mL/min/g). For luminal tumors on the other hand, only three tumors (8%) had a of MRFDG >20 μmol/min/100 g and all three had BF of >0.5 mL/min/g.

Several studies have shown that a BF metabolism mismatch, defined as high tumor glucose metabolism relative to BF, when compared with normal tissue, is associated with a more aggressive clinical behavior and therapeutic resistance (12, 18). Our data suggest that BF metabolism mismatch is more prevalent in the TN subtype when compared with luminal tumors. In the TN subtype, we observed greater heterogeneity in metabolism and BF, more frequent flow-metabolism mismatch, and no association between pretherapy imaging parameters and pCR. Prior work has shown that although the TN subtype is more likely to respond to systemic chemotherapy, patients with TN tumors that fail to respond to NC are more likely to relapse and die of their disease (2). Our findings in the TN subtype may shed light on some of the factors underlying this observation.

Metabolism and BF are both fundamentally important for normal cell survival and tissue viability. In normal tissue, autoregulatory mechanisms are responsible for the tight control of energy metabolism and BF (25), which tend to be highly correlated. This is not necessarily so with tumor cells. Both the vascular supply and energy metabolism is disorganized within tumor cells (26, 27), resulting in inefficient delivery and use of energy substrates and BF metabolism mismatch. Our data suggest that glucose metabolism and BF are relatively closely matched in the well-differentiated, luminal subtypes. As part of normal mammary function, differentiated breast epithelial cells proliferate and regress in response to the endocrine signaling that is part of female reproductive physiology (28, 29). One could hypothesize that the ability to match tissue perfusion to metabolic demand seen in most normal tissues

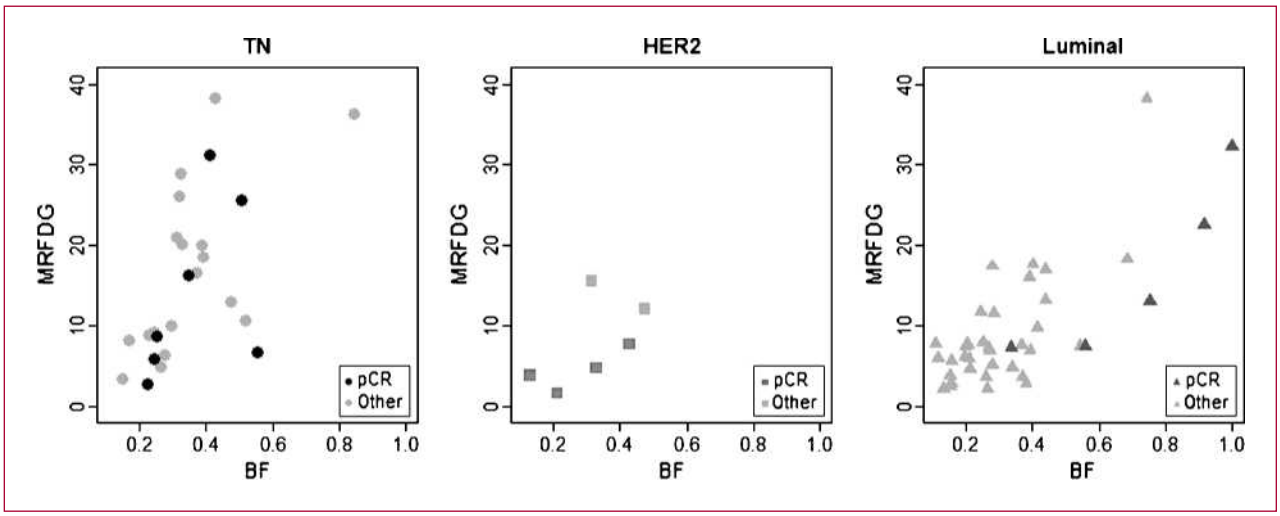

Fig. 4. MRFDG (μmol/min/100 g) and BF (mL/min/g) for each subtype. Light shaded symbols, nonresponders; dark shaded symbols, patients who achieved pCR. ●, pCR in TN tumors; ■, pCR in HER2 tumors; ▲, pCR in luminal tumors.

Published OnlineFirst May 11, 2010; DOI: 10.1158/1078-0432.CCR-10-0026

(24, 25, 30) is preserved in more differentiated forms of breast cancer.

The TN subtype is thought to be molecularly similar to the basal, myoepithelial component of the normal breast that does not respond to endocrine signaling and has a more mesenchymal and less epithelial subtype (33). Our data suggest that tumors of this cell type often have glucose metabolism that is of proportion to tumor perfusion which, compared with luminal tumors, is the result of higher rates of glucose metabolism without comparable increases in tumor perfusion. This could be the result of molecular stimuli supporting enhanced glycolysis (27), an inadequate blood supply (26), or a combination of the two. It is interesting to note that the same pattern of flow-metabolism mismatch that is prevalent in locally advanced TN breast cancers is also seen in ischemically stressed myocardium (30) and could reflect the more mesenchymal origins of many TN breast cancers. This might be the result of differential gene expression for TN for luminal tumors including factors known to affect glucose metabolism such as GLUT-1 and hexokinase. The observation of more frequent flow-metabolism mismatch in TN tumors also suggests the potential for biological therapies targeting tumor vasculature and metabolism, and highlights the potential of functional imaging to elucidate mechanisms of response and resistance to an expanding arsenal of targeted therapies in development.

FDG uptake increases with inflammation (31, 32), raising concern that the high MRFDG and BF observed in some tumors may be due to an inflammatory response induced by diagnostic breast biopsy rather than tumor glycolytic acitivity. FDG and [^{15}O]-water PET scans were done between 1 and 72 days after breast biopsy (median, 16 d). We found no evidence for an inflammatory response; the correlations between days since biopsy were 0.10 ($P > 0.3$) for both MRFDG and BF values, and the average MRFDG and BF for scans done within 7 days of biopsy were not different from the average for scans conducted >7 days after biopsy (t test P of >0.8 for both). We conclude that inflammation induced by the diagnostic breast biopsy has minimal influence on tumor glucose metabolism or BF as assessed by PET.

There are several limitations to our study. Ours is a retrospective analysis of prospectively acquired data with a relatively small number of patients. Determination of tumor subtype was based on IHC, which may not necessarily coincide with intrinsic subtype determined gene expression profiling (34). Future studies comparing tumor flow and metabolism measured by imaging to the intrinsic subtype assessed by gene expression arrays may shed more light on this observed phenomenon. Our sample sizes for the HER2 ($n = 6$) and luminal B ($n = 10$) subtypes were too small to attempt more than descriptive analysis. Over the course of this study, NC for LABC advanced with more frequent use of taxanes. Incorporation of HER2-targeted therapy, i.e., trastuzumab, was not routine before 2005 and the potential benefits of such biological therapy on pCR were not reflected in this analysis. Imaging parameters are macroscopic measures taken from the most metabolically active portion of the tumor and do not account for the heterogeneity that likely exists within these large tumors. Analysis using parametric imaging methods that can examine the heterogeneity of glucose metabolism and BF across the extent of the tumor may provide more insight.

In summary, we observed a difference in the rate of glucose metabolism and the relationship between glucose metabolism and tumor perfusion in luminal tumors versus TN tumors. Further examination of the relationship between tumor metabolism, perfusion, and gene expression may help explain these differences and may shed light on *in vivo* tumor biology and response to systemic therapy.

Disclosure of Potential Conflicts of Interest

No potential conflicts of interest were disclosed.

Grant Support

CA72064 and CA42045 (D.A. Mankoff), and CA015704 (B.F. Kurland).
The costs of publication of this article were defrayed in part by the payment of page charges. This article must therefore be hereby marked *advertisement* in accordance with 18 U.S.C. Section 1734 solely to indicate this fact.

Received 01/06/2010; revised 03/01/2010; accepted 03/21/2010; published OnlineFirst 05/11/2010.

References

1. Perou CM, Sorlie T, Eisen MB, et al. Molecular portraits of human breast tumors. Nature 2000;406:747–52.
2. Carey LA, Dees EC, Sawyer L, et al. The triple negative paradox: primary tumor chemosensitivity of breast cancer subtypes. Clin Cancer Res 2007;13:2329–34.
3. Sorlie T, Perou CM, Tibshirani R, et al. Gene Expression patterns of breast carcinomas distinguish tumor subclasses with clinical implications. Proc Natl Acad Sci U S A 2001;98:10869–74.
4. Rouzier R, Perou CM, Symmans WF, et al. Breast cancer molecular subtypes respond differently to preoperative chemotherapy. Clin Cancer Res 2005;11:5678–85.
5. Sorlie T, Tibshirani R, Parker J, et al. Repeated observation of breast tumor subtypes in independent gene expression data sets. Proc Natl Acad Sci U S A 2003;100:8418–23.
6. Cleater S, Heller W, Coombes R. Triple-negative breast cancer: therapeutic options. Lancet Oncol 2007;8:235–44.
7. Liedtke C, Mazouni C, Hess KR, et al. Response to neoadjuvant therapy and long-term survival in patients with triple-negative breast cancer. J Clin Oncol 2008;26:1275–81.
8. Keam B, Im S-A, Kim H-J, et al. Prognostic impact of clinicopathologic parameters in stage II/III breast cancer treated with neoadjuvant docetaxel and doxorubicin chemotherapy: paradoxical features of the triple negative breast cancer. BMC Cancer 2007:7.
9. Dunnwald LA, Gralow JR, Ellis GK, et al. Tumor metabolism and blood flow changes by positron emission tomography: relation to survival in patients treated with neoadjuvant chemotherapy for locally advanced breast cancer. J Clin Oncol 2008; 26:4449–57.

Published OnlineFirst May 11, 2010; DOI: 10.1158/1078-0432.CCR-10-0026

10. Mankoff DA, Dunnwald LA, Gralow JR, et al. Blood flow and metabolism in locally advanced breast cancer: relationship to response to therapy. J Nucl Med 2002;43:500–9.
11. Mankoff DA, Dunnwald LA, Gralow JR, et al. Change in blood flow and metabolism in locally advanced breast cancer treated with neoadjuvant chemotherapy. J Nucl Med 2003;44:1806–14.
12. Mankoff DA, Dunnwald LA, Partridge SC, Specht JM. Blood Flow-Metabolism Mismatch: Good for the Tumor, Bad for the Patient: commentary on Komar et al., p. 5511. Clin Cancer Res 2009;15:5294–6.
13. Komar G, Kauhanen KL, Seppanen M, et al. Decreased blood flow with increased metabolic activity: a novel sign of pancreatic tumor aggressiveness. Clin Cancer Res 2009;15:5511–7.
14. Eby P, Partridge SC, White S. Metabolic and vascular features of dynamic contrast-enhanced breast magnetic resonance imaging and (15)O-water positron emission tomography blood flow in breast cancer. Acad Radiol 2008;15:1246–54.
15. Chia S, Swain SM, Byrd DR, Mankoff DA. Locally advanced and inflammatory breast cancer. J Clin Oncol 2008;25:786–90.
16. Feldman LD, Hortobagyi GN, Buzdar AU, Ames FC, Blumenschein GR. Pathological assessment of response to induction chemotherapy in breast cancer. Cancer Res 1986;46:2578–81.
17. McCready D, Hortobagyi G, Kau S, Smith T, Buzdar A, Balch C. The prognostic significance of lymph node metastases after preoperative chemotherapy for locally advanced breast cancer. Arch Surg 1989; 124:21–5.
18. Miles KA, Williams RE. Warburg revisited: imaging tumour blood flow and metabolism. Cancer Imaging 2008;8:81–6.
19. Basu S, Chen W, Tchou J, et al. Comparison of triple-negative and estrogen receptor-positive/progesterone receptor positive/HER2-negative breast carcinoma using quantitative fluorine-18 flurodeoxyglucose/positron emission tomography imaging parameters. Cancer 2007;112:995–1000.
20. Sobin L, Fleming I. TNM classification of malignant tumors, fifth edition (1997): union Internationale Contre le Cancer and the American Joint Committee on Cancer. Cancer 1997;80:1803–4.
21. Sobin L, Wittekind C. TNM Classification of Malignant Tumors, 6th edition: International Union Against Cancer. 6th ed New York: Wiley-Liss; 2002.
22. Hamacher K, Coenen H, Stocklin G. Efficient stereospecific synthesis of no-carrier added 2-[18F]-fluoro-2-deoxy-D-glucose using aminopolyether supported nucleophilic substition. J Nucl Med 1986;27:235–8.
23. Lewellen T, Kohmyer S, Miyaoka R. Investigation of the count rate performance of the General Electric ADVANCE positron emission tomograph. IEEE Trans Nucl Sci 1995;42:1051–7.
24. Tseng J, Dunnwald LA, Schubert EK, et al. 18F-FDG kinetics in locally advanced breast cancer: correlation with tumor blood flow and changes in response to neoadjuvant chemotherapy. J Nucl Med 2004;45:1829–37.
25. Tune JD, Gorman MW, Feigl EO. Matching coronary blood flow to myocardial oxygen consumption. J Appl Physiol 2004;97:404–15.
26. Jain RK. Antiangiogenic therapy for cancer: current and emerging concepts. Oncology 2005;19:7–16.
27. Thompson CB, Bauer DE, Lum JJ, et al. How do cancer cells acquire the fuel needed to support cell growth? Cold Spring Harb Symp Quant Biol 2005;70:357–62.
28. Mallepel S, Krust A, Chambon P, et al. Paracrine signaling through the epithelial estrogen receptor α is required for proliferation and morphogenesis in the mammary gland. Proc Natl Acad Sci U S A 2006;103:2196–201.
29. Nandi S. Endocrine control of the mammary gland development and function in the C3H/H3 Crgl mouse. J Natl Cancer Inst 1958;21: 1039–63.
30. Schelbert HR. PET contribution to understanding normal and abnormal cardiac perfusion and metabolism. Ann Biomed Eng 2000;28: 922–9.
31. Basu S, Chryssikos T, Moghadam-Kia S, Zhuang H, Torigian DA, Alavi A. Positron emission tomography as a diagnostic tool in infection: present role and future possibilities. Semin Nucl Med 2009;39:36–51.
32. Zhuang H, Yu JQ, Alavi A. Applications of fluorodeoxyglucose-PET imaging in the detection of infection and inflammation and other benign disorders. Radiol Clin North Am 2005;43:121–34.
33. Fadare O, Tavassoli FA. Clinical and pathologic aspects of basal-like breast cancers. Nat Clin Pract Oncol 2008;5:149–59.
34. Parker JS, Mullins M, Cheang MCU, et al. Supervised risk predictor of breast cancer based on intrinsic subtypes. J Clin Oncol 2009;27: 1160–7.
35. Krak N, van der Hoeven J, Hoekstra O, et al. Blood flow and glucose metabolism in stage IV breast cancer; heterogeneity of response during chemotherapy. Mol Imaging Biol 2008;10:356–63.
36. Ellis GK, Green SJ, Russell CA, et al. SWOG 0012, a randomized phase III comparison of standard doxorubicin (A) and cyclophosphamide followed by weekly taclitaxel (T) versus weekly doxorubicin and daily oral cyclophosphamide plus G-CSF followed by weekly paclitaxel as neoadjuvant therapy for inflammatory and locally-advanced breast cancer. J Clin Oncol 2006;24:LBA 537.

AACR American Association for Cancer Research

Clinical Cancer Research

Tumor Metabolism and Blood Flow as Assessed by Positron Emission Tomography Varies by Tumor Subtype in Locally Advanced Breast Cancer

Jennifer M. Specht, Brenda F. Kurland, Susan K. Montgomery, et al.

Clin Cancer Res 2010;16:2803-2810. Published OnlineFirst May 11, 2010.